PERGAMON

International Journal of Heat and Mass Transfer 45 (2002) 4911–4924

International Journal of HEAT and MASS TRANSFER

www.elsevier.com/locate/ijhmt

Optimal tree-shaped networks for fluid flow in a disc-shaped body

W. Wechsatol [a], S. Lorente [b], A. Bejan [a,*]

[a] Department of Mechanical Engineering and Materials Science, Duke University, P.O. Box 90300, Durham, NC 27708-0300, USA
[b] Department of Civil Engineering, National Institute of Applied Sciences (INSA), 135 Avenue de Rangueil, Toulouse 31077, France

Received 11 June 2001; received in revised form 31 May 2002

Abstract

In this paper we consider the fundamental problem of how to design a flow path with minimum overall resistance between one point (O) and many points situated equidistantly on a circle centered at O. The flow may proceed in either direction, from the center to the perimeter, or from the perimeter to the center. This problem is an integral component of the electronics cooling problem of how to bathe and cool with a single stream of coolant a disc-shaped area or volume that generates heat at every point. The smallest length scale of the flow structure is fixed (d), and represents the distance between two flow ports on the circular perimeter. The paper documents a large number of optimized dendritic flow structures that occupy a disc-shaped area of radius R. The flow is laminar and fully developed in every tube. The complexity of each structure is indicated by the number of ducts (n_0) that reach the central point, the number of levels of confluence or branching between the center and the perimeter, and the number of branches or tributaries (e.g., doubling vs. tripling) at each level. The results show that as R/d increases and the overall size of the structure grows, the best performance is provided by increasingly more complex structures. The transition from one level of complexity to the next, higher one is abrupt. Generally, the use of fewer channels is better, e.g., using two branches at one point is better than using three branches. As the best designs become more complex, the difference between optimized competitors becomes small. These results emphasize the robustness of optimized tree-shaped networks for fluid flow.

Keywords: Constructal theory; Tree networks; Electronics cooling; Topology optimization; Dendritic; Flow geometry; Constructal design

1. Smaller scales demand greater complexity and optimization of construction

Thermal engineering is marching in step with other fields toward phenomena and devices at smaller and smaller scales. The engineering at microscales of only ten years ago is being renewed by developments at considerably smaller scales (meso, nano) in a revolution that is sweeping all fields. The cooling of electronics, which has inspired the fundamental problem proposed in this paper, is an excellent example of how engineering knowledge—mental and physical constructs—progresses toward smaller scales to make things more useful, and to pack finite-size spaces with more things that are useful.

In design, and in society in general, space is at a premium. This is why the interest in performance at smaller and smaller scales is natural, and will continue. This focus, however, misses an equally critical part of the picture. The devices engineered and touched by us—the contrivances that enlarge the sphere and enhance the capabilities of every human being—have scales that are comparable with ours, or are even larger. Full-scale devices are macroscopic. The miniaturization revolution means not only that the smallest identifiable volume element (the *elemental* system [1]) is becoming smaller, but also that larger and larger numbers of such elements must inhabit the macroscopic device that they serve.

* Corresponding author. Tel.: +1-919-660-5309; fax: +1-919-660-8963.
E-mail address: dalford@duke.edu (A. Bejan).

0017-9310/02/$ - see front matter
PII: S0017-9310(02)00211-9

Nomenclature

a, b	ratios, Eqs. (20) and (21)
A	area (m^2)
d	smallest, fixed peripheral length scale (m)
D	tube diameter (m)
f	dimensionless flow resistance, Eqs. (10) and (28)
g	dimensionless function, Eq. (18)
L	tube length (m)
$\dot{m}$	mass flow rate ($kg\,m\,s^{-1}$)
n	number of tubes
R	disc radius (m)
V	tube volume (m^3)
x, y	dimensions (m), Fig. 5

Greek symbols

α, β, γ	angles (rad), Figs. 2, 5–8, and 11–13
ΔP	pressure drop ($N\,m^{-2}$)
v	kinematic viscosity, ($m^2\,s^{-1}$)
ξ	ratio, x/y

Superscript

$\hat{()}$	dimensionless notation, Eq. (26)

Subscripts

i	rank of tube
min	minimum
p	tube touching the perimeter, Fig. 5
0	tube touching the center, Fig. 1
1, 2, ...	tubes positioned progressively closer to the perimeter

Each elemental volume "works" because it is accessed by electrical, heat and fluid currents. Each element must be connected to the macroscopic currents that flow into and out of the full-scale, macroscopic system. This necessity endows the system with structure (geometry, architecture, topology). The smaller the elements, and the larger their number, the greater the complexity of the structure. In design, miniaturization also means increasing complexity.

The driving force behind all these developments is the need for "better" performance from *our* point of view, at our scale, for our benefit. Needed are improvements in the global performance of the macroscopic system. Packing the system with smaller, more powerful and more numerous elemental systems is a necessary first step. The challenge is not only to find geometric arrangements to connect the currents that must access the elemental systems, but to *optimize* each connection such that, ultimately, each design choice is reflected in an increase in performance at the global level. To assemble more and more elements into complex structures, and to optimize (with global objective and space constraints) each connection means to *construct*.

In sum, hand in hand with greater engineering powers at smaller scales comes greater complexity and, especially, greater challenges to optimize the complex flow architecture—the internal connections—of the macroscopic system. The flow architecture is the result of the pursuit of global objective subject to global constraints. Numerous examples of optimized (i.e., deduced) flow structures from engineering and nature have been brought together under the title of constructal theory [1]. In this paper we propose the problem of designing a new flow structure with minimal resistance in a plane: the point–circle flow, or the flow connects the center of a disc with the disc perimeter. The flow may proceed from the center to the perimeter, or in the opposite direction.

We consider the point–circle flow construction at the same fundamental level that other flow constructions have been optimized in the past. For example, the structure with minimal resistance between two points is the straight path with constant cross-section (round cross-section for fluid flow in a duct). The optimized structure for flow between one point and an area or volume (an infinity of points) is shaped as a tree in which every geometric detail is deducible from the minimization of global resistance to flow.

Point–circle flows are already recognized as useful designs for electronics cooling [2]. In this paper we consider the optimization of the flow structure. We show that the optimal point–circle flow pattern depends on how small the elemental scale (d, Fig. 1) is relative to the macroscopic scale represented by the circle radius (R, Fig. 1). When d is comparable with R, the optimal point–circle flow consists of radial ducts. When d is much smaller than R, the optimal flow structure is shaped as a tree that covers the disc. The complexity of the tree increases in discrete steps as the elemental scale becomes progressively smaller, or R becomes larger (e.g., Fig. 9). In every case, that is for a given d/R ratio, every geometric feature of the flow structure is derived from the global maximization of flow performance, subject to global flow constraints.

We mentioned the cooling of electronics as the engineering field that served as inspiration for formulating the point–circle problem. Several fundamental problems of packing most cooling into fixed spaces [2–13] have

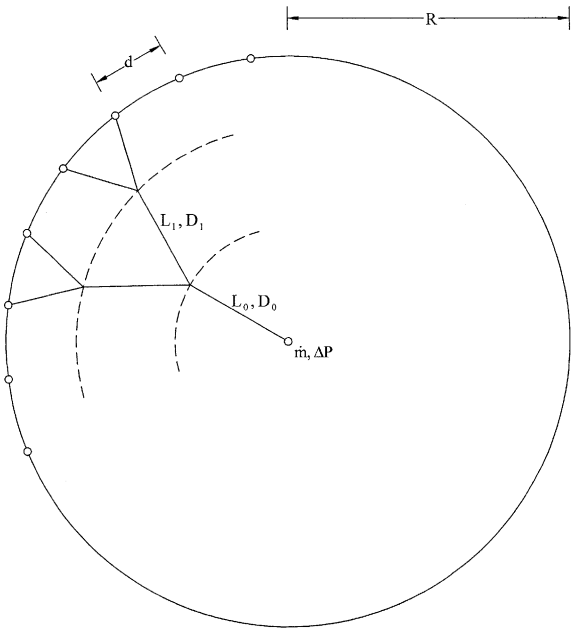

Fig. 1. Dendritic pattern of tubes connecting the center and the rim of a circular area.

served to identify the main statements of the objectives and constraints principle that generates optimal flow geometry in constructal design [1]. For example, the tree-shaped flows that have been optimized so far for the purpose of cooling spaces with volumetric heat generation, are flows that fill rectangular areas and parallel-epipedic volumes [1,14]. When the heat generating body is a cylinder, or a disc with insulated faces, the rectangular tree flows do not fit. The flow architectures for fluid and heat must be designed with the disc-shaped space as one of the global constraints.

One way to cool a disc-shaped domain that generates heat uniformly per unit area is by providing it with a stream of coolant that enters the disc through its center, bathes the disc, and exits through ports located on the disc perimeter. One part of the design problem is the point–circle (or center–perimeter) flow path that offers least resistance. This part is addressed in this paper.

2. Problem formulation

Consider the problem of designing dendritic paths of least flow resistance (or minimum ΔP) between the center of a disc-shaped area of radius R and points on its perimeter. The flow is between a point and a circle, and vice versa. It is not between one point and another point. The ducts are round tubes of several diameters (D_i) and lengths (L_i; $i = 0, 1, \ldots$). The volume occupied by all the tubes is fixed (this assumption is discussed more in Section 9). The flow regime in each tube is laminar and fully developed. We seek to optimize all the geometric details of a structure shaped as a tree, or, better, as a disc-shaped river basin or delta.

The flow rate $\dot{m}$ enters the flow structure through the center of the disc, and flows almost radially through tubes that become more numerous toward the rim of the disc. Outlet ports are positioned equidistantly along the rim. The flow may proceed in either direction, from the center to the rim, or from the rim toward the center. The main features of the structure are illustrated in Fig. 1, where for simplicity we assume dichotomy: pairing, or bifurcation at each node in the network. The optimal number of branches at each node may not be two: this is one of the questions to be considered in this study (Section 8).

The simplest setting for studying this problem is shown in Fig. 2. Several tubes (D_0, L_0) are positioned radially and equidistantly around the center port. The angle between two L_0 tubes is $\alpha = 2\pi/n_0$, where n_0 is the number of tubes (e.g., $n_0 = 4$ in Fig. 2). The flow rate through one L_0 tube is $\dot{m}_0 = \dot{m}/n_0$. Pairing means that there are $n_1 = 2n_0$ peripheral tubes of size (D_1, L_1). The flow rate through each peripheral tube is $\dot{m}_1 = \dot{m}/n_1$.To optimize the geometry of the flow structure means to select the aspect ratios (L_1/L_0, D_1/D_0) and the tube numbers such that the global resistance $\Delta P/\dot{m}$ is minimum. In Hagen–Poiseuille flow the resistance of tube (L_i, D_i) is

$$\frac{\Delta P_i}{\dot{m}_i} = \frac{128\nu}{\pi}\frac{L_i}{D_i^4} \tag{1}$$

Beginning with Murray's study of blood vessels [15], many studies have shown that there is an optimal size step (change in diameter) at each pairing node such that the global flow resistance is minimized,

$$\frac{D_{i+1}}{D_i} = 2^{-1/3} \tag{2}$$

In this notation, as in Figs. 1 and 2, the index i counts the tube sizes in the radial direction ($i = 0$ are the tubes that touch the center, and $i = p$ are the tubes that touch the perimeter). The optimal aspect ratio (2) is very robust: it does not depend on the lengths and geometric layout of the respective tubes [16]. We comment further on Murray's Eq. (2) in Section 9.

The newer aspect of the present problem is that the area over which the tubes may be arranged is constrained. In the simpler case of T- and Y-shaped arrangements of tubes, it was shown that the ratio of successive tube lengths can also be optimized [16]. In the present problem the Y-shaped construct of two L_1 tubes and one L_0 tube occupies the fixed area of the circle sector of angle α (Fig. 2, right). The pressure drop between the center and the ports on the rim is

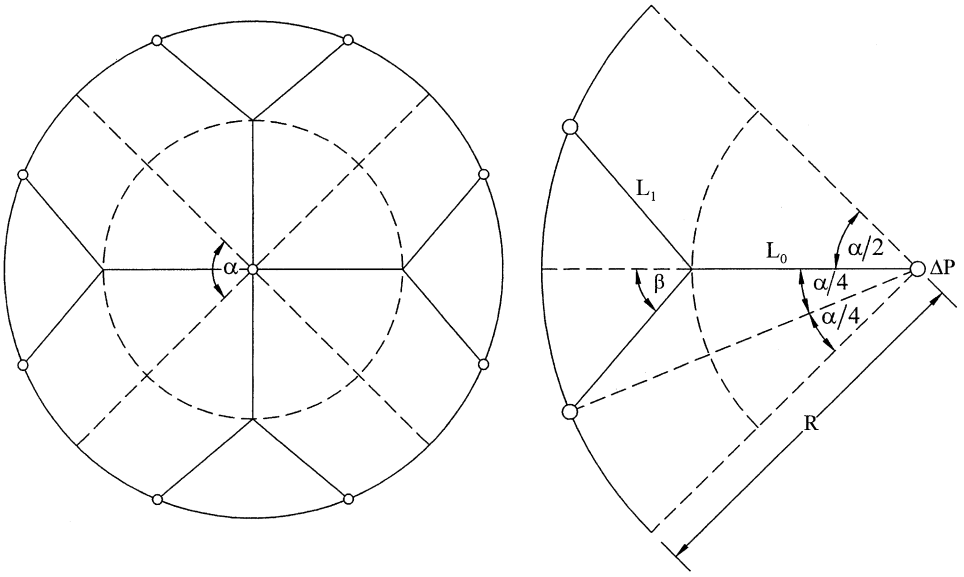

Fig. 2. Pattern with only one level of pairing or bifurcation, i.e., two tube sizes.

$$\Delta P = \Delta P_0 + \Delta P_1 = \dot{m}_0 \frac{128\nu}{\pi}\left(\frac{L_0}{D_0^4} + \frac{1}{2}\frac{L_1}{D_1^4}\right) \tag{3}$$

The volume occupied by the three tubes in the sector α is

$$V_\alpha = \frac{\pi}{4}\left(D_0^2 L_0 + 2D_1^2 L_1\right) \tag{4}$$

Using $D_1 = 2^{-1/3}D_0$, and eliminating D_0 between Eqs. (3) and (4) we arrive at

$$\Delta P = \dot{m}_0 \frac{8\pi\nu}{V_\alpha^2}\left(L_0 + 2^{1/3}L_1\right)^3 \tag{5}$$

So far we have made no assumptions regarding the orientation of the L_1 ducts for the purpose of minimizing ΔP. The geometry of the Y-shaped construct depends on the radial position of the node (i.e., the length L_0), or the angle β. Both L_0 and L_1 vary with β, when R is fixed:

$$L_0 = R\cos\left(\frac{\alpha}{4}\right) - R\frac{\sin(\alpha/4)}{\tan\beta} \tag{6}$$

$$L_1 = R\frac{\sin(\alpha/4)}{\sin\beta} \tag{7}$$

To minimize the flow resistance (5) means to minimize the expression $(L_0 + 2^{1/3}L_1)$ by varying β in accordance with Eqs. (6) and (7). The minimum resistance occurs when

$$\beta = 0.654 \text{ rad } (37.47^\circ) \tag{8}$$

It is remarkable that this angle does not depend on the sector angle α. It does not depend on the aspect ratio of the area that houses the construct. The minimized pressure drop that corresponds to this angle is

$$\Delta P = \dot{m}_0 \frac{8\pi\nu}{V_\alpha^2} R^3 \left[\cos\frac{\alpha}{4} + \sin\frac{\alpha}{4}\left(\frac{2^{1/3}}{\sin\beta} - \frac{1}{\tan\beta}\right)\right]^3 \tag{9}$$

The effect of the number of tubes becomes visible if we use $\alpha = 2\pi/n_0$, $\dot{m}_0 = \dot{m}/n_0$ and $V_\alpha = V/n_0$, where V is the total volume occupied by all the tubes. Eq. (9) becomes

$$\Delta P = \dot{m}\frac{8\pi\nu}{V^2} R^3 f(n_0) \tag{10}$$

where

$$f(n_0) = n_0\left[\cos\frac{\pi}{2n_0} + \sin\frac{\pi}{2n_0}\left(\frac{2^{1/3}}{\sin\beta} - \frac{1}{\tan\beta}\right)\right]^3 \tag{11}$$

The effect of n_0 is such that the global resistance increases as n_0 increases: $f(2) = 3.897$, $f(3) = 5.849$, $f(4) = 7.213$, $f(5) = 8.381$, $f(6) = 9.471$. The smallest number of central tubes ($n_0 = 2$) is not realistic because its corresponding length (L_0) is negative. The smallest realistic number is $n_0 = 3$, for which the corresponding lengths are $L_0 = 0.214R$ and $L_1 = 0.822R$. These aspect ratios and the optimal angle β are evident in the scale drawing shown in Fig. 3.

3. Fewer channels are better

The conclusion that a small number ($n_0 = 3$) of channels is the best way to connect the flow to one central point is important. It is akin to the recent demonstration that the best confluence (or branching) at a node is represented by dichotomy (pairing, bifurcation) [1]. Dichotomy is the well known geometric feature of all natural dendritic flows. Likewise, the flow of a river

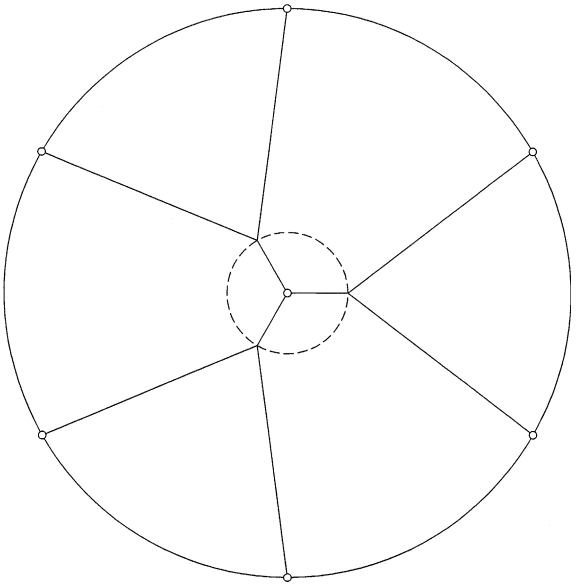

Fig. 3. The minimum-resistance flow structure when there is only one level of pairing or bifurcation.

delta starts with two or, maximum, three branches. The flow of a river delta is biased (tilted) in one direction by the slope of the terrain, unlike the pattern of Fig. 3. Radially unbiased dendritic patterns have been simulated by Chen [17], who injected water into a narrow parallel-plates space occupied by glycerin.

The minimization of flow resistance in a plane calls for simplicity in structure. The smallest number of channels is the best, and that number decreases as more constraints limit the freedom of the flow. In summary, the smallest numbers are (Fig. 4):

3. when the point flow has access to all the directions around that point (Fig. 4a)
2. when the point flow is biased in one direction by the larger stream (Fig. 4b),
1. when the point flow has access to only one direction (Fig. 4c); in this case, the resistance of the single and straight channel is less than the resistance of two channels in parallel, which have the same total volume.

The last two cases can be proven based on simple analysis. Further proof is provided by the numerical solutions presented in Section 8. As an extension of Fig. 4, we can expect that in a three-dimensional structure the best (smallest) number for channels out of (or into) a single point is 4, and that the best number of branches (or tributaries) for a stream is 3.

4. More complex radial dendrites

The imposed, global length scales of the flow pattern are not only the total extent (R, Fig. 1) but also the smallest distance between the points (ports) serviced by the flow structure (d, Fig. 1). The fixed smallest length scale is a characteristic of all dendritic flows, engineered or natural [1]. Diffusion governs the flow beyond the densest points, that is, at length scales smaller than d. In

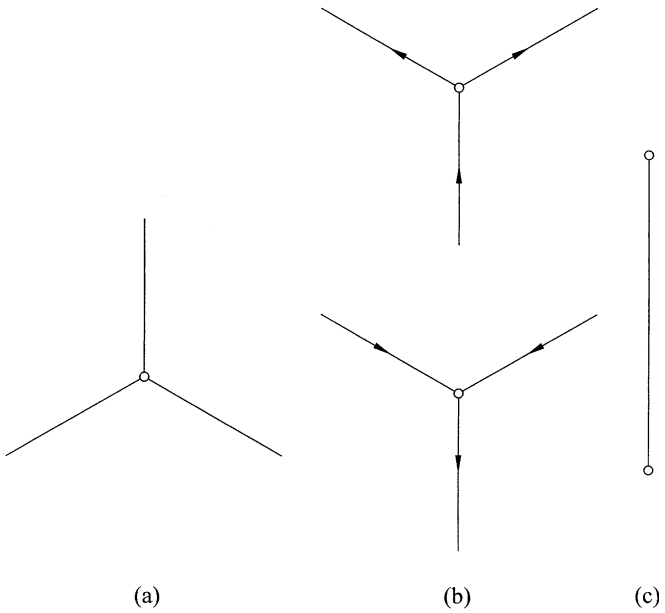

Fig. 4. The best (smallest) number of channels to or from one point in a plane.

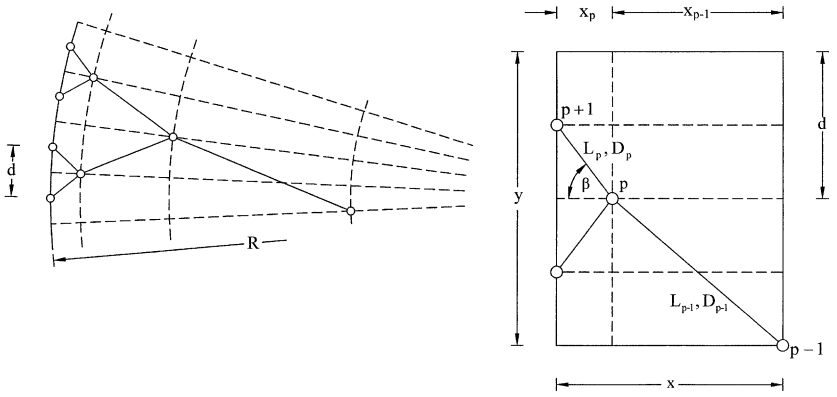

Fig. 5. Rectangular element near the rim of the dendritic pattern, when $R \gg d$.

this way, the flow of Fig. 1 connects the central point to the entire rim area of length $2\pi R$ and thickness d. In an engineered structure such as the supply of water or other goods from one central point, the rim represents the circle of consumers, where the territory represented by one consumer is of order d^2.

When d is smaller than but comparable with R, the best structure has only one level of pairing or branching (3 inner nodes), as in Fig. 3. When d is even larger, say between R and $2R$, nodes are not even necessary: the best way is to connect the central point to three equally spaced points around it. The angle between two adjacent ducts would be 120°.

Much more challenging is the case of a territory so large that the diffusion scale d is much smaller than R. This case is essential because all natural flows grow in size, if space is available: consequently, most radial dendrites are characterized by $R \gg d$, where d is fixed, and R increases in time. In such cases the number (p) of levels of pairing or bifurcation is not fixed. This number is an additional degree of freedom that can be selected such that the overall flow resistance is minimum. We can expect the optimal number of pairings to increase as R increases.

5. Pairings near the periphery

On the right side of Fig. 2 we saw that the area element that houses one Y-shaped construct (pairing, bifurcation) is a circular segment, i.e., a curvilinear triangle. When the pairing number is greater than one, the Y-shaped constructs that do not touch the center (source, sink) are housed by curvilinear rectangles. When R is considerably larger than d, the curvilinear rectangles that are located closer to the rim look progressively more like true rectangles.

This trend is illustrated in Fig. 5. We focus on one area element near the periphery, and assume that it is a rectangle. We seek the optimal architecture (aspect ratios) such that the flow resistance of the element is minimum, when the elemental area and tube volume are fixed. In other words, we pass the design of the rectangular system through the optimization steps outlined in Section 2 for one of the central sectors.

The size of the element ($A = xy$) is fixed. We know that A is of order d^2, but we do not know the best shape of A, i.e., the aspect ratio

$$\xi = \frac{x}{y} \tag{12}$$

The second degree of freedom of the rectangular structure is the relative position of the internal node. This variable is represented by the angle β.

The third degree of freedom is the tube diameters ratio D_p/D_{p-1}. According to Eq. (2), the optimal value is $2^{-1/3}$, regardless of the tube lengths (L_p, L_{p-1}) and their relative positions. The minimized flow resistance of the rectangular construct is obtained through a change in notation in Eqs. (4) and (5),

$$\Delta P_p = \dot{m}_{p-1} \frac{8\pi\nu}{V_p^2} \left(L_{p-1} + 2^{1/3} L_p\right)^3 \tag{13}$$

$$V_p = \frac{\pi}{4}\left(D_{p-1}^2 L_{p-1} + 2D_p^2 L_p\right) \tag{14}$$

The pressure drop ΔP_p is measured between node $(p-1)$ and the periphery $(p+1)$, i.e., ΔP_p is centered on node p. In this formulation V_p and $\dot{m}_{p-1}$ are the total tube volume and the total flow rate through node p. The tube lengths can be expressed in terms of the degrees of freedom (ξ, β) and constraints (A, V_p)

$$L_p = \frac{y}{4\sin\beta} \tag{15}$$

$$L_{p-1} = \left[\left(\frac{y}{2}\right)^2 + \left(x - \frac{y/4}{\tan\beta}\right)^2\right]^{1/2} \tag{16}$$

where $x = (\xi A)^{1/2}$ and $y = (A/\xi)^{1/2}$. Eq. (13) becomes

$$\Delta P_p = \dot{m}_p \frac{8\pi\nu}{V_p^2} A^{3/2} g^3 \tag{17}$$

where

$$g(\xi,\beta) = \left[\frac{1}{4\xi} + \left(\xi^{1/2} - \frac{1}{4\xi^{1/2}\tan\beta}\right)^2\right]^{1/2} + \frac{2^{1/3}}{4\xi^{1/2}\sin\beta} \tag{18}$$

The function g can be minimized with respect to both ξ and β:

$$g_{\min} = 1.324 \quad \text{at } \xi = 0.7656,\ \beta = 0.927 \text{ rad } (53.1^\circ) \tag{19}$$

In summary, the optimal D_p/D_{p-1}, ratio and the ξ and β values reported above represent the optimized architecture of the peripheral area element highlighted in Fig. 5. This design is valid when the element is approximately rectangular. The ξ and β values can be used to calculate other geometric ratios of the element, for example, the distances between successive pairings,

$$\frac{x_p}{x_{p-1}} = a = 0.325 \tag{20}$$

and the successive tube lengths,

$$\frac{L_p}{L_{p-1}} = b = 0.409 \tag{21}$$

All the elemental scales are proportional to the elemental spacing d, for example

$$\frac{x_p}{d} = 0.375, \quad \frac{L_p}{d} = 0.625 \tag{22}$$

If, as we proceed from the periphery toward the center, we approximate all the area constructs as rectangles, the distance from the periphery to the center is

$$R = \sum_{i=0}^{p} x_i = \frac{x_p(1-a^{p+1})}{(1-a)a^p} \tag{23}$$

Eq. (23) dictates the approximate number of pairing levels (p) when the elemental scale (d, or x_p) and the global scale (R) of the structure are known.

The overall flow resistance encountered by the stream ($\dot{m}_0$) between the periphery and the center of the disk is obtained by summing $(p+1)$ pressure drops of the type shown in Eq. (1),

$$\Delta P = \sum_{i=0}^{p} \Delta P_i = \dot{m}_0 \frac{128\nu}{\pi} \frac{L_p}{D_p^4} \left(2^{-4/3}b\right)^p \frac{1-\left(2^{1/3}b\right)^{p+1}}{1-2^{1/3}b} \tag{24}$$

The total volume of all the tubes in the structure is

$$V = \sum_{i=0}^{p} 2^i \frac{\pi}{4} D_i^2 L_i = \frac{\pi}{4} D_p^2 L_p \frac{1-\left(2^{1/3}b\right)^{p+1}}{\left(2^{-2/3}b\right)^p (1-2^{1/3}b)} \tag{25}$$

The elemental tube diameter (D_p) is assumed fixed, along with the other dimensions of the peripheral element. In this case Eq. (25) establishes a one-to-one relationship between V and p.

6. Two or more levels of branching

Eqs. (20) and (21) show that when there are many levels of branching or confluence (Fig. 5), the optimized area elements become smaller in sizeable steps as we approach the periphery. This trend contradicts the message of Fig. 3, which shows that when there is only one branching level the peripheral length scale (L_1) is greater than the central scale (L_0). To decide which trend is correct when the number of branching levels is moderately greater than 1, we performed the analysis of Section 2 for structures with two levels of branching, or pairing.

Fig. 6 shows the resulting optimized structure when, as in Fig. 3, the central region has only three ducts ($n_0 = 3$). This optimized geometry is represented by the lengths and angles reported in the top line ($n_0 = 3$) of Table 1. Note that all the lengths have been nondimensionalized by using R as reference,

$$\left(\hat{L}_i, \hat{x}_i\right) = (L_i, x_i)/R \tag{26}$$

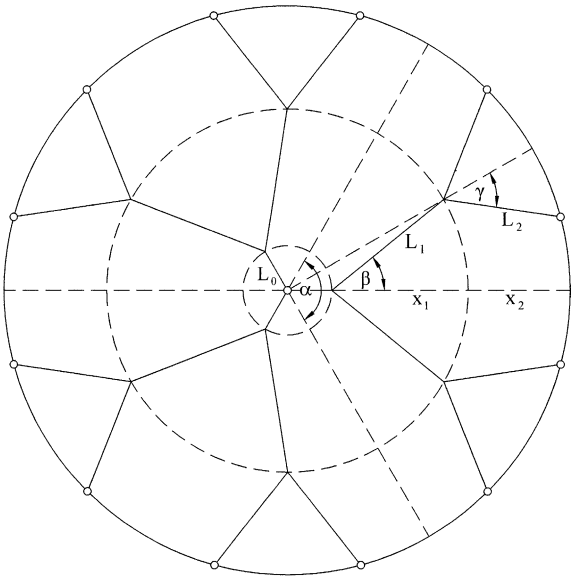

Fig. 6. The optimized flow structure with two levels of pairing and $n_0 = 3$.

Table 1
The optimized geometric features of flow structures with two levels of pairing (e.g., $n_0 = 3$ in Fig. 6)

n_0	β		γ		$\widehat{L}_0$	$\widehat{L}_1$	$\widehat{L}_2$	$\hat{x}_1$	$\hat{x}_2$	f
	deg	rad	deg	rad						
3	38.85	0.6783	36.77	0.6420	0.157	0.509	0.432	0.482	0.361	9.82
4	38.64	0.6747	39.78	0.6946	0.337	0.464	0.305	0.420	0.243	11.10
5	38.31	0.6689	41.65	0.7272	0.458	0.408	0.235	0.359	0.183	12.16
6	38.08	0.6648	42.96	0.7501	0.543	0.358	0.192	0.312	0.145	13.16
7	37.93	0.6623	43.95	0.7674	0.607	0.318	0.161	0.273	0.120	14.13
8	37.83	0.6605	44.73	0.7810	0.655	0.286	0.139	0.243	0.102	15.10
9	37.75	0.6591	45.34	0.7917	0.693	0.258	0.123	0.218	0.089	16.07
10	37.70	0.6583	45.85	0.8006	0.724	0.236	0.109	0.198	0.078	17.03
11	37.66	0.6576	46.28	0.8081	0.749	0.217	0.099	0.181	0.070	18.00
12	37.63	0.6570	46.63	0.8142	0.770	0.200	0.090	0.167	0.063	18.98
13	37.61	0.6567	46.94	0.8196	0.788	0.186	0.083	0.154	0.058	19.95
14	37.59	0.6563	47.21	0.8243	0.803	0.174	0.076	0.144	0.053	20.93
15	37.57	0.6557	47.44	0.8283	0.816	0.163	0.071	0.134	0.050	21.91
16	37.56	0.6555	47.65	0.8316	0.828	0.153	0.066	0.126	0.046	22.88

The f value is the minimum of the function

$$f = n_0\left(\widehat{L}_0 + 2^{1/3}\widehat{L}_1 + 2^{2/3}\widehat{L}_2\right)^3 \tag{27}$$

which is proportional to the overall flow resistance,

$$\Delta P = 8\pi\nu\dot{m}\frac{R^3}{V^2}f \tag{28}$$

The flow rate $\dot{m}$ is the total flow rate, and $\dot{m}_0 = \dot{m}/n_0$ is the flow rate through a single L_0 tube.

The structure of Fig. 6 begins to bridge the gap between Fig. 3 and the optimization rules of Eqs. (20) and (21). Note that in Fig. 6 the central duct (L_0) is sensibly shorter than the next, post-bifurcation duct (L_1). This is in qualitative agreement with the features of Fig. 3. The next two ducts show that $L_1 > L_2$. This is the feature anticipated in Eq. (21). It does represent a shift from increasing lengths ($L_1/L_0 > 1$, as in Fig. 3) to decreasing lengths ($L_p/L_{p-1} < 1$, as in Eq. (21)).

Table 1 shows the geometric features of optimized structures with two levels of pairing, when the number of central tubes (n_0) increases above 3. The pressure drop factor f increases monotonically with n_0, and indicates that the simplest structure ($n_0 = 3$) offers the smallest global resistance to flow. The table also shows that the proportionalities anticipated in Eqs. (20) and (21) are approached closely as n_0 increases. For example, when $n_0 = 16$, the ratios between the peripheral lengths are $x_2/x_1 = 0.365$ and $L_2/L_1 = 0.431$, which come close to Eqs. (20) and (21), respectively.

We took this optimization work to the next level of complexity, which is the structure with three levels of pairing. Fig. 7 is a scale drawing of the $n_0 = 3$ case, the dimensions of which are listed in the top line of Table 2. For a given n_0, the structure is characterized by four tube lengths (L_0, L_1, L_2, L_3) and three angles (β, γ, ϕ).

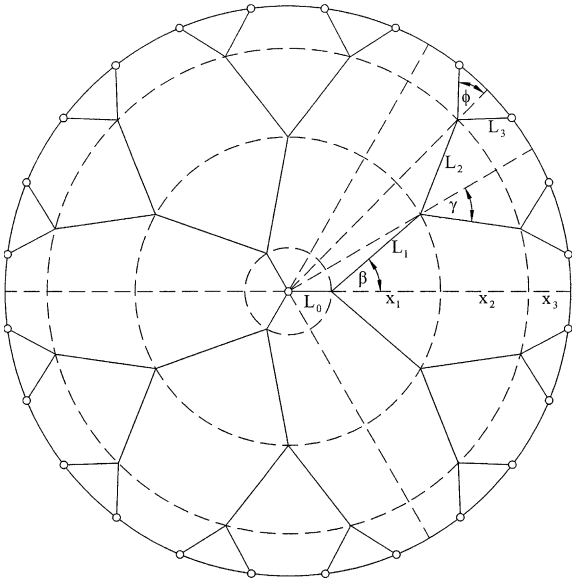

Fig. 7. The optimized flow structure with three levels of pairing and $n_0 = 3$.

The pressure drop factor f is defined as in Eq. (28), and is given by

$$f = n_0\left(\widehat{L}_0 + 2^{1/3}\widehat{L}_1 + 2^{2/3}\widehat{L}_2 + 2\widehat{L}_3\right)^3 \tag{29}$$

The table shows that f increases monotonically with n_0, and that the lowest resistance occurs when $n_0 = 3$.

The optimized ratios of lengths near the periphery, Eqs. (20) and (21), are approached by the results of Table 2 as n_0 increases. For example, when $n_0 = 3$ the ratios are $L_3/L_2 = 0.526$ and $x_3/x_2 = 0.477$. When $n_0 = 8$, the corresponding ratios have the values 0.465

Table 2
The optimized geometric features of flow structures with three levels of pairing (e.g., $n_0 = 3$ in Fig. 7)

n_0	β		γ		ϕ		$\widehat{L}_0$	$\widehat{L}_1$	$\widehat{L}_2$	$\widehat{L}_3$	$\hat{x}_1$	$\hat{x}_2$	$\hat{x}_3$	f
	deg	rad	deg	rad	deg	rad								
3	40.6	0.709	36.79	0.642	42.39	0.740	0.153	0.416	0.368	0.194	0.388	0.311	0.148	13.44
4	39.19	0.684	39.53	0.690	45.61	0.796	0.308	0.410	0.276	0.137	0.370	0.223	0.099	14.54
5	38.5	0.672	41.4	0.723	47.9	0.836	0.425	0.375	0.219	0.106	0.330	0.172	0.073	15.44
6	38.2	0.667	42.8	0.747	49.6	0.866	0.512	0.337	0.181	0.086	0.292	0.138	0.058	16.31
7	38	0.663	43.8	0.765	50.9	0.889	0.578	0.303	0.154	0.072	0.260	0.116	0.046	17.17
8	37.9	0.662	44.6	0.779	51.9	0.906	0.629	0.274	0.134	0.062	0.232	0.099	0.040	18.04

and 0.399, which are closer to the values anticipated in the limit of nearly rectangular peripheral area elements (Fig. 5 and Eqs. (20) and (21)).

It can be verified that the agreement improves when the structure has four levels of pairing. Fig. 8 shows the optimized structure for $n_0 = 3$, and Table 3 reports all the geometric features for $n_0 = 3, \ldots, 8$. The angles β, γ, ϕ and θ are defined on Fig. 8.

In summary, the analytical optimization developed based on Fig. 5 is supported by case-by-case optimized structures with two, three and four levels of pairing (Tables 1–3). The analytical results of Section 5 are more accurate (i.e., more appropriate) for more complex structures, i.e., structures with more central tubes and more levels of pairing.

7. When branching is beneficial

All the tree-shaped flows developed so far represent *design*–optimal geometric form with purpose. Every dendrite took shape on our piece of paper because we sought the minimization of the resistance to fluid flow between one central point and many points on a circle circumscribed to the center. We developed several classes of optimized dendritic patterns: trees with one level of pairings (Fig. 3), two levels (Fig. 6), three levels (Fig. 7), and four levels (Fig. 8). Which dendritic pattern is better?

The answer depends on what is fixed. We continue to rely on the view that the smallest length scale of the flow pattern—the elemental scale—is known and fixed [1]. In Section 5 this length scale was the distance (d) between two adjacent points on the circle. Let us also assume that the radius of the circle (R) is fixed. This means that the number of points on the circle (N) is fixed. It is also reasonable to assume that the total volume of the tubes installed on the R-fixed disc is also a constant.

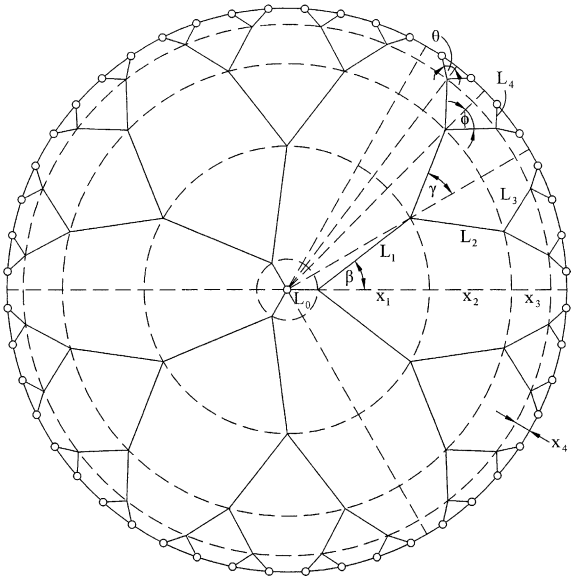

Fig. 8. The optimized flow structure with four levels of pairing and $n_0 = 3$.

Table 3
The optimized geometric features of flow structures with four levels of pairing (e.g., $n_0 = 3$ in Fig. 8)

n_0	β	γ	ϕ	θ	$\widehat{L}_0$	$\widehat{L}_1$	$\widehat{L}_2$	$\widehat{L}_3$	$\widehat{L}_4$	$\hat{x}_1$	$\hat{x}_2$	$\hat{x}_3$	$\hat{x}_4$	f
3	37.5	38.1	43.1	49.8	0.109	0.420	0.337	0.180	0.086	0.402	0.292	0.139	0.058	16.04
4	37.5	39.9	45.9	52.7	0.275	0.407	0.263	0.131	0.062	0.372	0.219	0.096	0.038	17.10
5	37.5	41.6	48	54.9	0.400	0.371	0.212	0.103	0.048	0.330	0.170	0.072	0.028	17.92
6	37.5	42.8	49.6	56.5	0.493	0.333	0.177	0.084	0.039	0.291	0.138	0.057	0.021	18.67
7	37.5	43.8	50.9	57.7	0.562	0.300	0.151	0.071	0.033	0.259	0.115	0.046	0.018	19.44
8	37.5	44.6	51.9	58.7	0.615	0.271	0.132	0.061	0.029	0.232	0.099	0.039	0.015	20.23

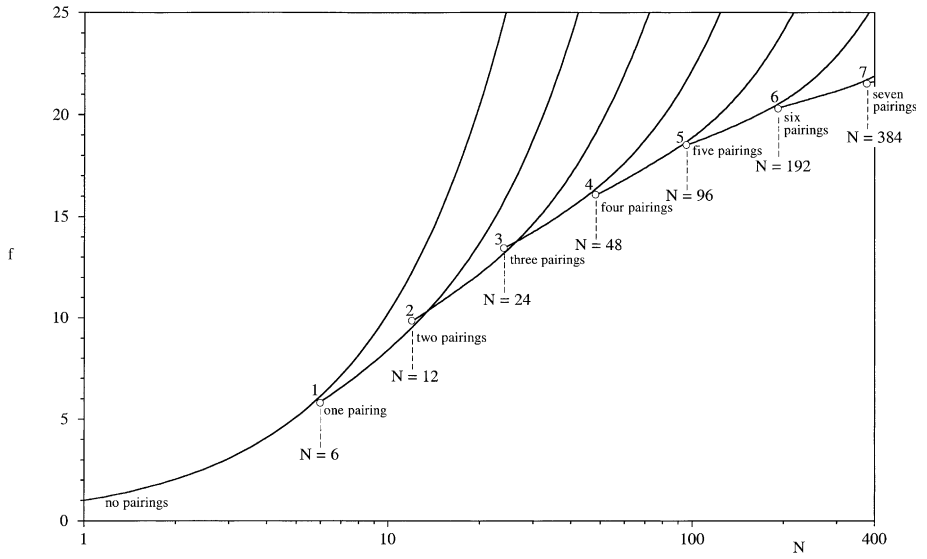

Fig. 9. The effect of the number of levels of pairing on the global flow resistance (f) when the number of points on the circle (N) is fixed, and the radius (R) and the total tube volume (V) are fixed.

Under these circumstances, formulas such as Eq. (28) show that the global flow resistance of the tree construct ($\Delta P/\dot{m}$) varies proportionally with f, while the other factors are constant. The flow pattern with less global resistance is the one with the lower f value. This is why we took special care in calculating the f values reported in Tables 1–3. These values are plotted in Fig. 9, where we have used continuous curves for each class (number of levels of pairing) even though N is an integer. The leftmost curve corresponds to purely radial flow (no pairings): one can show that this curve is represented by the line $f = N$. Each of the subsequent $f(N)$ curves is almost a straight line when plotted on a graph with linear scales in f and N.

The smallest f corresponds to $N = 1$, or a single radial tube between the center and a point on the circle. The next highest f belongs to $N = 2$. These banal cases fall outside the class of flows that form the subject of this paper (point–circle flows). They are point-point flows, and are certainly not relevant to the cooling of a disc-shaped body that generates heat.

Fig. 9 is instructive for additional reasons. We read this figure vertically, at $N =$ constant. One conclusion is that pairing, or branching is a useful feature if N is sufficiently large (greater than 6). The larger the N value, the more likely the need to design more levels of pairings into the flow structure. If the number of points on the rim of the structure (N) increases, then the flow structure with minimal flow resistance becomes more complex. Complexity increases because N increases, and because the number of pairing levels increases. Complexity is the mechanism by which the dendritic flow assures its minimal resistance status. Optimized complexity is the design principle.

If we think of fixed rims (R) with more and more points (N), then the search for minimal flow resistance between the rim and the center requires discrete changes in the structure that covers the disc. To start with, N has to be large enough for an optimized structure with one or more pairings to exist. These starting N values (6, 12, 24, ...) are indicated with circles in Fig. 9. As the structures become more complex, these circles describe a nearly smooth curve in the semilogarithmic plot of Fig. 9. When there are three or more levels of pairing, the circles indicate the *transition* from one type of structure to the next type with one more level of branching. This transition, or competition between competing flow structures, is analogous to the transition and flow pattern selection in Bénard convection. In the vicinity of each circle in Fig. 9, the designer can choose between two structures, as both have nearly the same resistance. These choices are illustrated in Fig. 10, which shows the two dentritic structures that compete in the vicinity of points 3 and 4 of Fig. 9.

The transition from structures with one pairing to structures with two levels of pairing does not occur at the smallest N where two levels of pairing exist. Note that the curves labeled (1) and (2) in Fig. 9 intersect where N is larger than 12, namely at $N = 13.75$. This means that the choice is between two designs with $N = 16$: the design with one level of pairing and $n_0 = 8$, and the design with two levels of pairing and $n_0 = 4$. The latter is slightly better. Note also that curve (1) is the same as Eq. (11), in which $n_0 = N/2$. There is also an intersection between curves (2) and (3), which occurs at $N = 27.52$. The choice between structures with two, three and four levels of pairing is illustrated in Fig. 10.

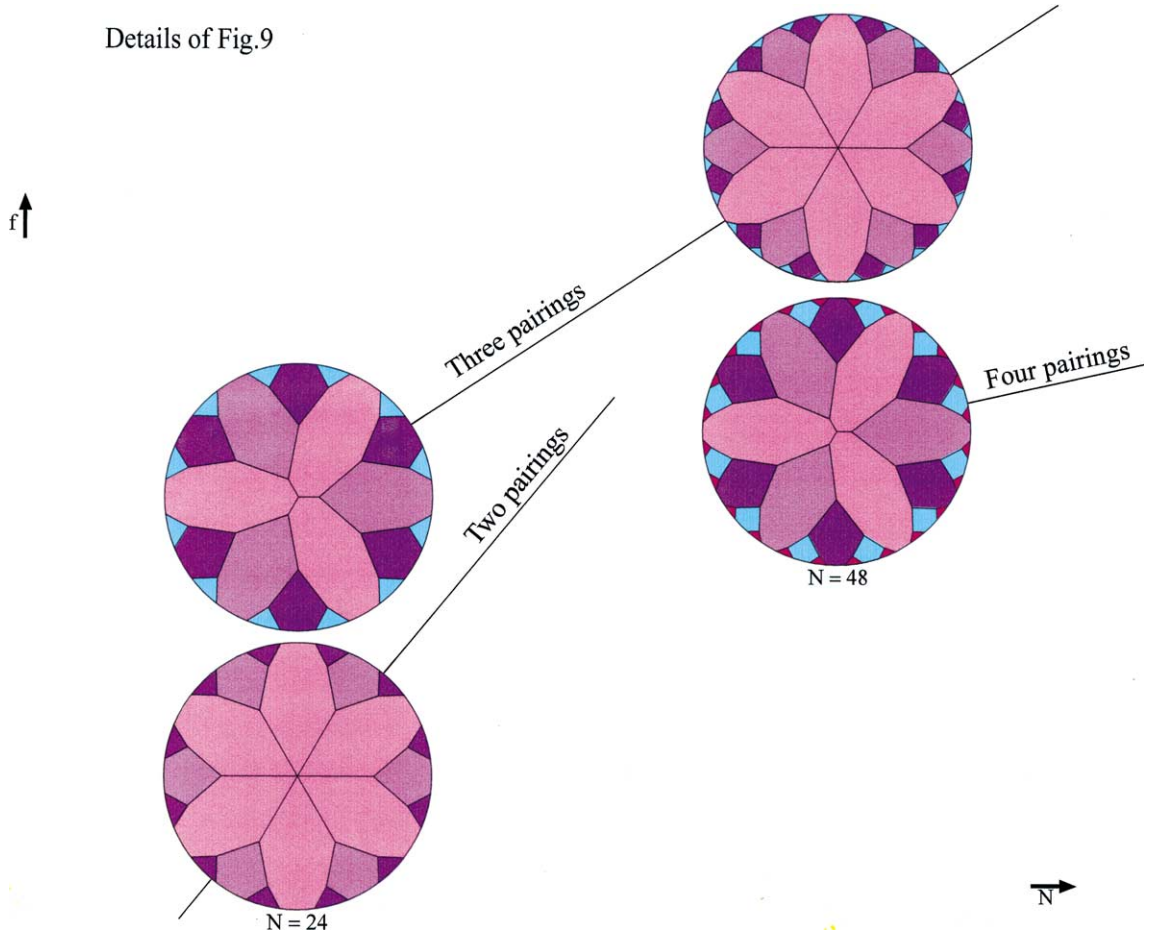

Fig. 10. The transition from one tree structure to one with one more level of pairing, as the flow resistance (f) is minimized while N increases.

8. Three branches instead of two

An increasingly large number of points (N) on the circular perimeter (R) can be supplied with fluid at the same rate by increasing the number of pairing levels (Figs. 9 and 10), or by increasing the number of branches at each branching level. We investigated this second alternative by optimizing flow structures with three branches instead of two.

Fig. 11 is a scale drawing of the optimized flow architecture where there are three central tubes ($n_0 = 3$), one branching level, and three branches on every central tube. The number of points on the rim ($N = 9$) are positioned equidistantly. The total volume of all the tubes is fixed. The structure has three degrees of freedom when the disc size (R) is fixed, namely, the angle β and the tube diameter ratios D_1/D_0 and $D_{1'}/D_0$. The flow-resistance minimization procedure is the same as in the preceding sections, and is not described here. Noteworthy is that the two outer branches ($L_{1'}$, $D_{1'}$) are longer than the inner branch (L_1, D_1). The optimized structure is characterized completely by

$$L_0/R = 0.360, \quad L_1/R = 0.640, \quad L_{1'}/R = 0.760,$$
$$\beta = 57.7°, \quad D_1/D_0 = 0.68, \quad D_{1'}/D_0 = 0.71 \qquad (30)$$

The minimized overall flow resistance is $f = 8.24$, where f has the same meaning as in Eq. (28). Note that this point ($f = 8.24$, $N = 9$) falls above the "one pairing" curve plotted in Fig. 9. There is no point at $N = 9$ on that curve; the closest points are $N = 8$ ($n_0 = 4$) and $N = 10$ ($n_0 = 5$). Even so, the f value of the $N = 9$ structure of Fig. 11 suggests that structures with three branches are only marginally inferior to structures with two branches.

We took a closer look at this suggestion by optimizing two structure types that have exactly the same number of ports on the rim, $N = 12$. Both have only one level of branching. The optimized structure reported in Fig. 12 has two branches on every central tube ($n_0 = 6$),

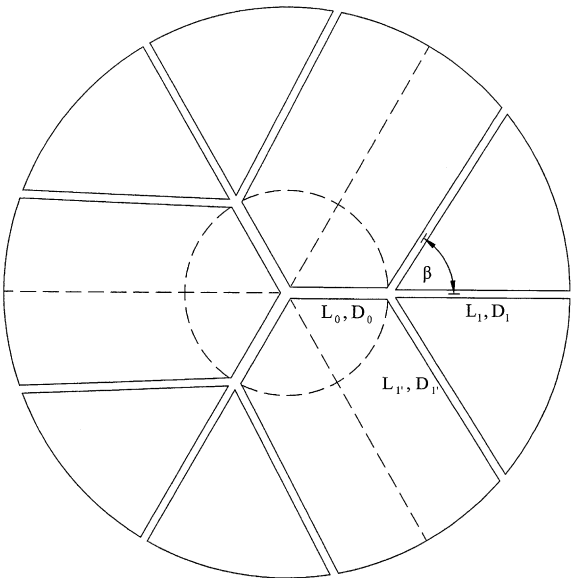

Fig. 11. The optimized flow structure with one level of branching, and three branches on every central tube ($n_0 = 3$, $N = 9$).

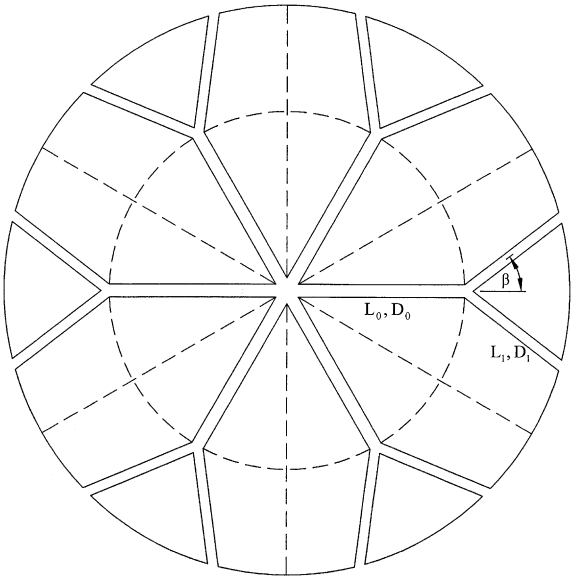

Fig. 12. The optimized flow structure with one level of branching and two branches on every central tube ($n_0 = 6$, $N = 12$).

and the global flow resistance $f = 9.471$. The competing flow structure shown in Fig. 13 has three branches on every central tube ($n_0 = 4$), and the resistance $f = 9.602$. In conclusion, in this particular case the use of three branches instead of two leads to a 1.4% increase in the overall flow resistance. Pairing is better than tripling.

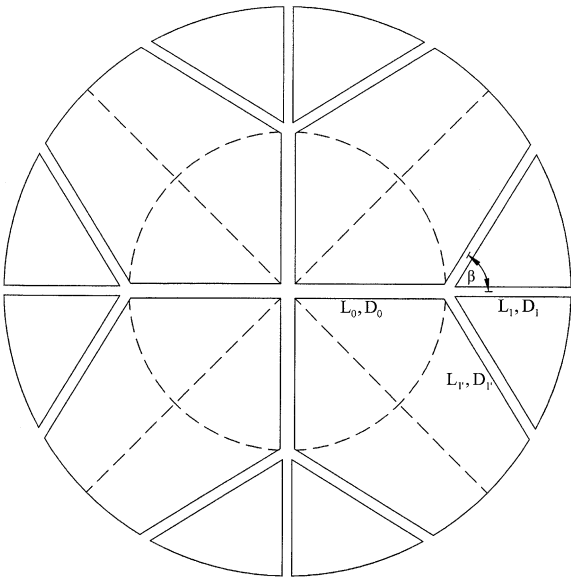

Fig. 13. The optimized flow structure with one level of branching and three branches on every central tube ($n_0 = 4$, $N = 12$).

The more practical conclusion is that two optimized structures that are visually different (Figs. 12 and 13) perform at nearly the same level.

9. Concluding remarks

The use of three branches instead of two can be advantageous when the R and d constraints are such that the number of peripheral parts (N) cannot be accommodated by a pairing sequence, regardless of the number of pairing levels. To illustrate this design opportunity, consider a flow structure that must have $N = 36$ ports on the perimeter. According to the results shown in Fig. 9, two flow structures generated by the pairing rule are possible:

$$\begin{array}{ll} \text{one pairing level } (n_0 = 18) & f = 21.62 \\ \text{two pairing levels } (n_0 = 9) & f = 16.07 \end{array} \tag{31}$$

If, on the other hand, we use three branches at each level of complexity increase, and if we optimize every geometric detail as in all the designs exhibited until now, we find that there are flow structures that can be generated based on the tripling rule:

$$\begin{array}{ll} \text{one tripling level } (n_0 = 12) & f = 17.58 \\ \text{two tripling levels } (n_0 = 4) & f = 15.56 \end{array} \tag{32}$$

Results (31) and (32) show that the designs with three branches perform better; specifically, the overall flow resistance of the structure with two tripling levels

($f = 15.56$) is 3.2% smaller than the flow resistance of the structure with two pairing levels ($f = 16.07$). This conclusion strengthens what we wrote in the preceding paragraph. Note that the curve for three pairings and $N = 36$ in Fig. 9 suggests a value ($f = 14.99$) that is even lower than the f value achieved with two tripling levels. The catch is that a structure with $N = 36$ and three pairing levels would require the use of a number of central channels that is not an integer ($n_0 = 4.5$). In conclusion, as more and more complex structures compete on the minimum-resistance envelope of all the possible designs, some flow structures with three branches are the best when structures with two branches are not possible. On the envelope, competing designs perform similarly even though they appear to be different (e.g., doubling vs. tripling). We see once again that optimized tree-shaped flows are robust.

The work that we reported was based on several simplifying assumptions, which had the merit of simplifying the design without hurting the fundamental character of the questions that we pursued. For example, we assumed that each duct is round and the flow regime is laminar and fully developed. We also neglected pressure-drop losses due to entrance effects at points of confluence and bifurcation. Future treatments of this fundamental problem may consider the effect of variable cross-sectional areas of ducts, and the effect of periodically fully developed flow and heat transfer.

The results—the optimized tree-shaped flow structures—are valid for other duct cross-sections with fully developed laminar flow. In such cases, the pressure drops are described by proportionalities of the same type as in Eq. (1), with the appropriate hydraulic diameter in place of D_i. In other words, the optimized diameter ratios that we reported in this paper are also valid for the ratios between successive hydraulic diameters, provided that the cross-sectional shape is preserved.

Trends such as the recommended transitions to better and more complex flow structures (Figs. 9 and 10), and the robustness of the optimized complex structures can be expected in further extensions of this work. For example, in an earlier study we found that if the laminar flow assumption is replaced by the assumption of fully developed turbulent duct flow, the same optimization opportunities exist (e.g., ratios of diameters, lengths, optimal layouts in space) even though the actual numerical values (e.g., aspect ratios) may not be the same as in laminar flow [16]. This is why we submit this optimization of the point–circle flow structure as a fundamental first step. The same method can be used in conjunction with more realistic models, and the generation of optimized geometry should follow the steps that we outlined.

We use this opportunity to draw attention to an important observation regarding the minimization of pumping power subject to flow volume constraint. Murray's optimized diameter ratio (2) came originally [18] from the minimization of an objective function that had two terms: (i) the fluid pumping power, and (ii) the "cost" of the blood volume, which was proportional to the volume of all the flow tubes. For example, in the case of a single tube with diameter D and fully developed laminar flow, term (i) is proportional to D^{-4}, and term (ii) is proportional to D^2. Both terms vary as D varies, and from the minimization of the linear combination of (i) and (ii) resulted the optimal D for the tube, or the optimal ratio of tube diameters for bifurcated tubes. The observation is that this optimization procedure is equivalent to minimizing (i) alone, but under the assumption that (ii) is constrained, cf. the method of Lagrange multipliers. This is why in contemporary studies of complex flow networks the optimization is based routinely on (i) as objective function, and (ii) as constraint.

How realistic is (ii) as a constraint? In physiology, this constraint is very important because mass (space, weight) comes at a premium. Every unit mass on the animal requires a proportional cost in spent exergy (food intake, motive power). For example, this proportionality is very clear in the case of animal flight [1, p. 239]. In the cooling of electronics, the invocation of (ii) is justified on the same basis: the maximization of the use of space is the objective. In other words, space that is allocated in an existing design to cooling ducts could have been used better, for example, for the packing (compacting) of additional electronics. The mechanism that generates future designs is the constructal principle: the maximization of global performance in a constrained but morphing flow structure, in a process where the visible result is geometric form (e.g., flow architecture).

Acknowledgements

The work reported in this paper was supported by the National Science Foundation.

References

[1] A. Bejan, Shape and Structure, from Engineering to Nature, Cambridge University Press, Cambridge, UK, 2000.
[2] D.V. Pence, Improved thermal efficiency and temperature uniformity using fractal-like branching channel networks, in: G.P. Celata, V.P. Carey, M. Groll, I. Tanasawa, G. Zummo (Eds.), Heat Transfer and Transport Phenomena, Begell House, New York, 2000, pp. 142–148.
[3] S.J. Kim, S.W. Lee, Air Cooling Technology for Electronic Equipment, CRC Press, Boca Raton, FL, 1995.
[4] G.P. Peterson, A. Ortega, Thermal control of electronic equipment and devices, Adv. Heat Transfer 20 (1990) 181–314.

[5] W. Aung (Ed.), Cooling Technology for Electronic Equipment, Hemisphere, New York, 1988.
[6] W. Li, S. Kakac, F.F. Hatay, R. Oskay, Experimental study of unsteady forced convection in a duct with and without arrays of block-like electronic components, Wärme-und Stoffübertragung 28 (1993) 69–79.
[7] S.H. Kim, N.K. Anand, Laminar developing flow and heat transfer between a series of parallel plates with surface mounted discrete heat sources, Int. J. Heat Mass Transfer 37 (1994) 2231–2244.
[8] G. Guglielmini, E. Nanei, G. Tanda, Natural convection and radiation heat transfer from staggered vertical fins, Int. J. Heat Mass Transfer 30 (1987) 1941–1948.
[9] A. Bar-Cohen, W.M. Rohsenow, Thermally optimum spacing of vertical, natural convection cooled, parallel plates, J. Heat Transfer 106 (1984) 116–123.
[10] N.K. Anand, S.H. Kim, L.S. Fletcher, The effect of plate spacing on free convection between heated parallel plates, J. Heat Transfer 114 (1992) 515–518.
[11] S. Kakac, H. Yüncü, K. Hijikata (Eds.), Cooling of Electronic Systems, Kluwer, Dordrecht, The Netherlands, 1994.
[12] H.H. Bau, Optimization of conduits shape in micro heat exchangers, Int. J. Heat Mass Transfer 41 (1998) 2717–2723.
[13] T.M. Harms, M. Kazmierczak, F.M. Gerner, A. Hölke, H.T. Henderson, J. Pilchowski, K. Baker, Experimental investigation of heat transfer and pressure drop through deep microchannels in a (110) silicon substrate, ASME HTD 351 (1997) 347–357.
[14] A. Bejan, Constructal-theory network of conducting paths for cooling a heat generating volume, Int. J. Heat Mass Transfer 40 (1997) 799–816.
[15] C.D. Murray, The physiological principle of minimum work, in the vascular system, and the cost of blood-volume, Proc. Acad. Nat. Sci. 12 (1926) 207–214.
[16] A. Bejan, L.A.O. Rocha, S. Lorente, Thermodynamic optimization of geometry: T- and Y-shaped constructs of fluid streams, Int. J. Therm. Sci. 39 (2000) 949–960.
[17] J.-D. Chen, Radial viscous fingering patterns in Hele-Shaw cells, Exp. Fluids 5 (1987) 363–371.
[18] C.D. Murray, The physiological principle of minimal work, in the vascular system, and the cost of blood-volume, Proc. Acad. Nat. Sci. 12 (1926) 207–214.